Mo-Si-B Alloy Development

J. H. Schneibel

Oak Ridge National Laboratory, Metals and Ceramics Division, P. O. Box 2008, Oak Ridge, TN 37831-6115

E-mail: schneibeljh@ornl.gov; Telephone: (865) 576-4644; Fax: (865) 574-7659

ABSTRACT

Alloys consisting of the phases α-Mo (Mo solid solution), Mo_3Si, and Mo_5SiB_2 ("T2") were fabricated by ingot and powder metallurgy. A novel powder-metallurgical processing technique was developed which allows the fabrication of silicide alloys with a continuous α-Mo matrix. In these alloys the relatively ductile and tough α-Mo matrix acts as a "binder" for brittle silicide particles. An alloy processed in this manner with the nominal composition Mo-15Si-10B exhibited a room temperature fracture toughness of 14 MPa $m^{1/2}$. By controlling the composition and microstructure, other properties such as fracture toughness and creep strength can be optimized. A powder-metallurgically processed alloy with the composition Mo-16.8Si-8.4B (at. %) exhibited a weight loss of only 5 mg/cm^2 after 1 day at 1300°C in air. Partial substitution of Mo with Nb increased the creep strength at temperatures ranging from 1200 to 1400˚C significantly. Similar to the oxidation and fracture toughness properties, the microstructural scale and morphology have a pronounced influence on the creep strength.

INTRODUCTION

Nickel-base superalloys have outstanding oxidation and mechanical properties at elevated temperatures, but their service temperatures are inherently limited to temperatures around 1000˚C. In order to increase the thermodynamic efficiency of Fossil Energy systems, materials capable of much higher temperatures are needed. One approach, pioneered in Japan, focuses on precious metal based superalloys [1]. While these superalloys have simple fcc-based crystal structures, which allow significant plastic deformation, a heavy price is paid in terms of mass density and cost. An alternative approach is based on oxidation resistant intermetallic compounds which have lower densities and are less costly, but which are inherently brittle. In particular, silicide intermetallics, which can have outstanding oxidation resistance, are being considered. A prime example is $MoSi_2$ that is widely used in heating elements for resistance furnaces. Its good oxidation resistance is due to the formation of a protective silica glass scale. However, $MoSi_2$ is very brittle with a room temperature fracture toughness on the order of 3 MPa $m^{1/2}$ [2]. Also, it becomes very weak at high temperatures [2]. If the Si concentration is reduced below that of $MoSi_2$, phases such as Mo_5Si_3, Mo_3Si, and α-Mo (Mo solid solution) form. These phases will have a lower oxidation resistance, but they may potentially impart greater fracture toughness, particularly in the case of α-Mo. Two main alloy systems have been examined to date. In the first one, which was pioneered by Akinc and collaborators [3], intermetallic alloys consisting of Mo_5Si_3, the T2 phase Mo_5SiB_2, and the A15 phase Mo_3Si were investigated. These types of alloys are indicated in the schematic ternary phase diagram in Fig. 1. They exhibit excellent oxidation resistance at elevated temperatures (e.g., 1300°C). The boron additions are crucial for providing the observed oxidation resistance [4,5], as already hinted at in an early study of the ternary Mo-Si-B phase diagram by Nowotny et al. [6]. In the second system, which was pioneered by Berczik et al. [7,8], alloys consisting of α-Mo, Mo_3Si, and T2 were investigated. While these alloys are not as oxidation resistant as Mo_5Si_3-T2-Mo_3Si alloys, they contain a ductile phase, α-Mo. Depending on its volume fraction and distribution, the α-Mo can improve the room and high temperature fracture toughness significantly. The fracture toughness will increase with increasing α-Mo volume fraction and, for a given α-Mo volume fraction, will be higher if the α-Mo forms as a continuous matrix instead of individual particles [9]. Clearly, then, the optimization of Mo-Si-B alloys requires a trade-off between fracture toughness on the one hand, and oxidation resistance on the other.

Another issue is the creep resistance of these types of alloys. Akinc et al. have already shown that Mo_5Si_3-based alloys exhibit excellent creep resistance [3]. Mo_3Si, $(Cr,Mo)_3Si$, and the T2 phase are all very strong at elevated temperatures [10-12]. Since it can be safely assumed that the creep strength of α-Mo is lower than that of Mo_3Si and T2, the creep strength of Mo-Mo_3Si-T2 alloys is likely to depend on the α-Mo volume fraction. It will also depend sensitively on the microstructural morphology - if the α-Mo is distributed as a continuous matrix or "binder" phase instead of isolated particles, the creep strength will be low. In addition, as commonly observed in creep, the grain or phase size will play an important factor – generally, the creep strength tends to increase with increasing grain or phase size. The competing requirements for optimum

oxidation resistance, fracture toughness, and creep strength are schematically shown in Fig. 2. Using the Mo-Si-B system we will illustrate the issues raised in Fig. 2. It should also be noted that several aspects of Mo-Si-B alloys are also being examined within the Department of Energy/Basic Energy Sciences Synthesis&Processing Center on "Design and Synthesis of Ultrahigh-Temperature Intermetallics." For example, the significant thermal expansion anisotropy of Mo_5Si_3, which gives rise to profuse microcracking during processing, has now been understood based on first-principles calculations [13]. Based on these calculations alloying additions for Mo_5Si_3 have been found which reduce the ratio of the thermal expansions in the c- and a-directions from 2 to 1.2 [14].
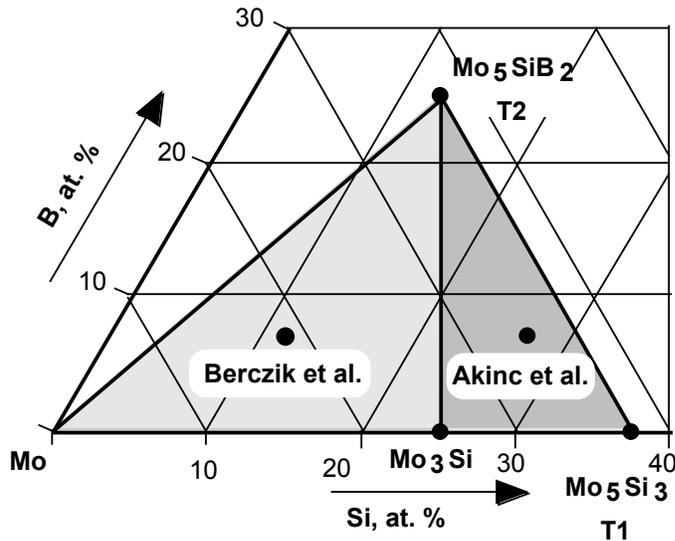

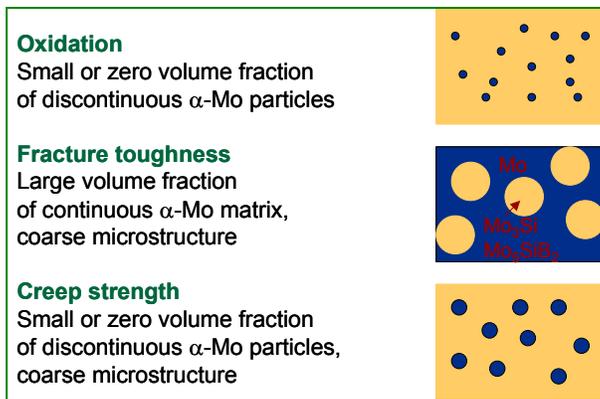Figure 1: Schematic illustration of the Mo-rich section of the ternary Mo-Si-B phase diagram.

Figure 2. Schematic illustration of the phase volume fractions and microstructures needed to satisfy competing requirements.

EXPERIMENTAL

The alloys in this work were prepared by arc-melting of elemental starting materials in a partial pressure of argon (70 kPa) on a water-cooled copper hearth. The purity of the starting materials Mo, Si and B was 99.95, 99.99, and 99.5 wt%, respectively. Unless stated otherwise, alloy compositions will from now on be stated in at. %. The alloys were re-melted several times in order to improve their homogeneity. Sometimes the alloys were allowed to solidify in elongated water-cooled Cu molds, in other cases they were drop-cast into cylindrical water-cooled copper molds with diameters of 12.5 or 25 mm. After casting, the alloys were usually annealed for 24 hours at 1600°C in vacuum at a pressure of approximately 10^{-4} Pa. Several as-cast alloys were crushed into powders with sizes ranging from 20 to 230 µm. They were mixed with various amounts of Mo powder (2-8 µm) and consolidated either by hot isostatic pressing in sealed Nb cans or by uniaxial hot-pressing in a graphite hot press. In a novel approach to be described in more detail in the experimental section, the surface of

Mo-Si-B particles (which were obtained by crushing castings into powder) was "coated" with a thin (10 μm) layer of Mo by removing Si via vacuum annealing

Microstructural examination was carried out by optical microscopy as well as scanning electron microscopy (SEM). Metallography specimens were prepared by grinding, mechanical polishing, and etching in Murakami's etch. The phases were identified by a combination of energy dispersive spectroscopy (EDS) in an SEM, by wavelength-dispersive spectroscopy (microprobe), and powder x-ray diffraction.

In order to assess the oxidation resistance of the Mo-Si-B alloys, screening tests were carried out. Small coupons (typically $10 \times 10 \times 1$ mm) were weighed and annealed for 1 day in an air furnace at 1300°C such that all their surfaces were oxidized. Their oxidation resistance was determined by dividing their weight change after annealing by their surface area.

Fracture toughness values were estimated from the energy dissipation during controlled crack growth of chevron-notched specimens [15].

Compression specimens with a diameter of 3 mm and a height of 6 mm were electro-discharge machined. Their creep strengths were evaluated from constant displacement rate tests in flowing argon at temperatures ranging from 1200 to 1400°C in an Instron testing machine equipped with a $MoSi_2$ furnace.

RESULTS AND DISCUSSION

OXIDATION RESISTANCE

Figure 3 illustrates the influence of the microstructure on the oxidation resistance. The alloy on the left was processed by mixing Mo-20Si-10B (at. %) powder particles (obtained by crushing a casting with that composition) with Mo powder. The nominal composition after mixing was Mo-16.8Si-8.4B (at. %). The Mo occurred in the form of large, elongated particles. The alloy on the right had the same nominal composition, but it was consolidated directly from powder obtained from a Mo-16.8Si-8.4B casting, without adding any Mo powder. Since the α-Mo in this alloy is present in the form of small particles, the oxidation resistance of this alloy is much better than that of the one on the left, see Fig. 3.
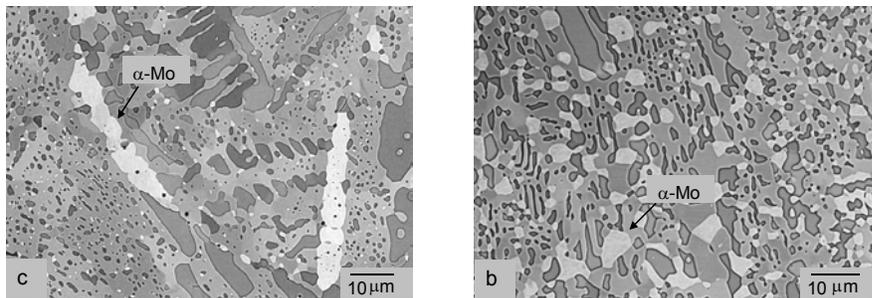

Figure 3. The oxidation resistance depends sensitively on the microstructure

Weight loss 220 g/cm² (1day/1300C/air)

Weight loss 5.7 mg/cm² (1day/1300C/air)

FRACTURE TOUGHNESS

For a given volume fraction of a toughening phase, the fracture toughness is greatest when this phase is distributed continuously, acting as a "binder" for brittle silicide particles, similar to the microstructure of WC-Co [9]. Melting and casting, or powder-metallurgical processing starting with Mo-Si-B castings cannot deliver such microstructures, and a new technique had therefore to be developed. The Mo-Si system is unique in the sense that, depending on the oxygen partial pressure, either Mo or Si can be removed from its surfaces. During oxidation in air, Mo is removed as MoO_3, the surfaces are enriched in Si, and a protective SiO_2 scale develops. During annealing in vacuum, silicon instead of Mo is oxidized. Because of the low partial pressure of oxygen, SiO forms instead of SiO_2. SiO is volatile and is removed. As a consequence, the surface becomes a Mo solid solution. This approach proved to be very useful to effectively "coat" Mo-Si-B powder particles with a thin (10 μm) film of α-Mo. The reactions occurring during the annealing, as well as a cross-section through an annealed powder particle, are shown in Fig. 4.

"Coating" of silicide powders with Mo
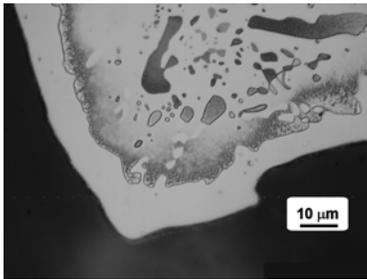
Mo-20Si-10B
powder particle
after 16 h at 1600°C
in vacuum

Figure 4. Formation of a thin α-Mo layer on a Mo-20Si-10B particle during annealing in vacuum.

$$Mo_3Si + 1/2 O_2 \rightarrow SiO\uparrow + 3\ Mo$$
$$Mo_5SiB_2 + 1/2\ O_2 \rightarrow SiO\uparrow + 2\ Mo_2B + Mo$$
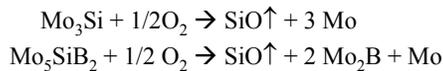
The kinetics of the reaction follows a power law – the thickness of the α-Mo layer grows proportional to time$^{1/2}$. This is not surprising since the removal of the silicon involves diffusion of Si through the α-Mo layer to the surface where it is removed as SiO. Since the α-Mo layer increases progressively in thickness, the rate at which the Si is removed slows down with time.

Figure 5 shows the microstructure of silicide material processed in this manner. An α-Mo layer was produced on Mo-20Si-10B powder particles which were then consolidated by hot isostatic pressing in a Nb can at 1600°C for 2 h at a pressure of 30 ksi. The nominal composition of the consolidated alloy was Mo-15Si-10B. As shown in Fig. 5, the room temperature fracture toughness of this material is quite high, namely, 14 MPa m$^{1/2}$, as measured with flexure tests carried out with chevron-notched specimens [15]. This value is higher than that of a cast and annealed alloy (Mo-12Si-8.5B) with a higher α-Mo volume fraction of approximately 40%, which has a fracture toughness of 9.5 MPa m$^{1/2}$ (determined by the same technique). The reasons for the high fracture toughness of the PM material are two-fold. First, the α-Mo is distributed continuously and a propagating crack can therefore not avoid it by going around it. Second, the microstructural size of the α-Mo ligaments is large and this also enhances the fracture toughness.
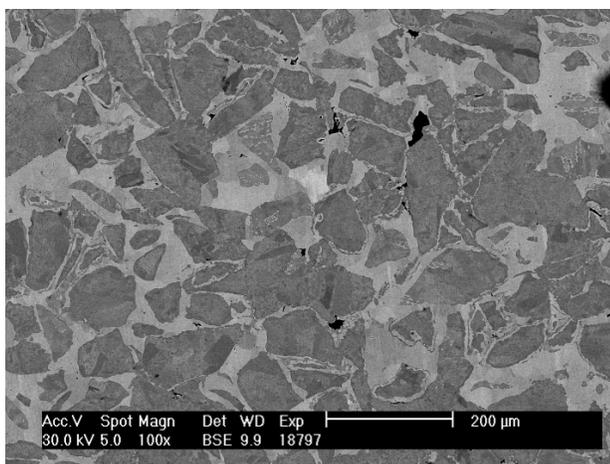
Figure 5. The microstructure of hot isostatically pressed silicide with the nominal composition Mo-15Si-10B illustrating the continuous nature of the α-Mo matrix (bright contrast).

CREEP STRENGTH

Slow high-temperature compression tests with a constant crosshead displacement rate were carried out in flowing argon. The initial strain rate was 1×10^{-5} s^{-1}. A quasi-steady state flow stress (steady-state creep strength) was typically reached after a plastic strain of about 2%. Sometimes a gradual load drop occurred after a strain of a few percent. The creep strength was estimated as the engineering stress for a plastic strain of 2%. Alloys based on Mo-12Si-8.5B in which the Mo was partially replaced by W or Nb were cast and annealed (24h/1600˚C/Vacuum). The alloying additions did not change the scale and morphology of the microstructure significantly. However, with tungsten, a small amount of a Mo_5Si_3-based phase is observed. Table I shows electron microprobe data for the partitioning of the W or Nb in the different phases. Tungsten partitions primarily to the α-Mo. Consistent with its atomic size (which is almost identical to that of Mo) and its relative low solubility in the Mo_3Si and Mo_5SiB_2 phases, W does not improve the creep strength significantly (Fig. 6). Niobium, on the other hand, which partitions strongly to all phases and has a much larger atomic size than Mo, causes substantial solid solution strengthening.

Figure 7 illustrates the pronounced influence of the morphology and scale of the microstructure on the creep strength. As a base line, the creep strength of cast and annealed Mo-12Si-8.5B is indicated. When the α-Mo in Mo-16.8Si-8.4B is fine and discontinuous (see right-hand side of Fig. 3), the creep strength at 1400˚C is poor. This is consistent with the fine microstructure and the abundance of high-diffusivity paths for mass transport, such as grain and interface boundaries. At "lower" temperatures the strength of this alloy is high – presumably Hall-Petch strengthening, characteristic of fine-grained microstructures at lower temperatures, occurs. An alloy with the same nominal composition, but a much coarser microstructure is much stronger in creep (see also the microstructure on the left-hand side of Fig. 3).

Table I. Composition of the phases in Mo-19.5W-12Si-8.5B and Mo-19.5Nb-12Si-8.5B.

Note that the B concentrations tend to be overestimated.

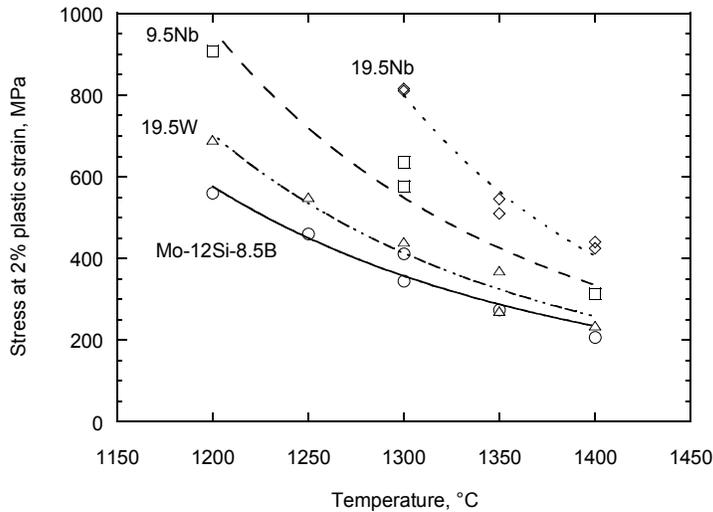| Specimen	Phase	Mo	Nb	W	Si	B
Mo-19.5Nb-12Si-8.5B	α-Mo	82.1	15.7		2.2	
	Mo_3Si	59.6	17.2		23.2	
	Mo_5SiB_2	35.2	21.0		11.5	32.2
Mo-19.5W-12Si-8.5B	α-Mo	60.9		33.1	0.4	5.6
	Mo_3Si	69.7		4.5	23.7	2.1
	Mo_5SiB_2	39.0		8.7	9.1	43.3
	Mo_5Si_3	57.1		3.9	35.7	3.3

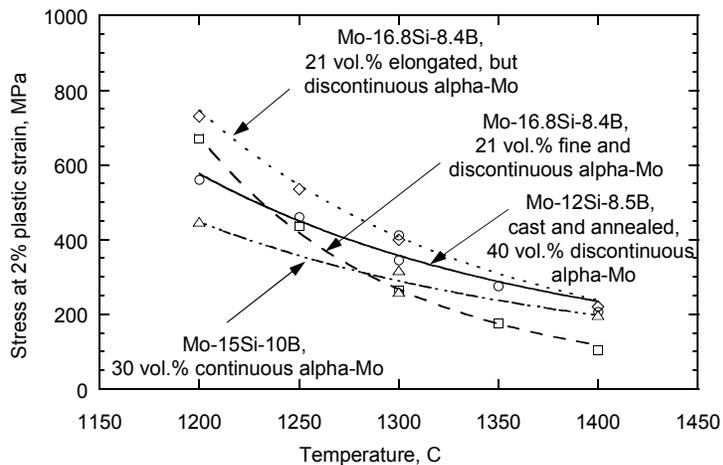Figure 6. Creep strength of cast and annealed molybdenum silicides.

Figure 7. Creep strength of Mo-Si-B alloys with different α-Mo volume fractions, size scales, and morphologies. The creep strength of cast and annealed Mo-12Si-8.5B is indicated for reference.

CONCLUSIONS

Boron-containing silicides with compositions in the Mo-Mo$_3$Si-Mo$_5$SiB$_2$ three-phase field can be quite resistant to oxidation. When the volume fraction and the continuity of the α-Mo solid solution phase is reduced, the oxidation resistance increases. However, at the same time the room temperature fracture toughness decreases. This is no surprise since both Mo$_3$Si and Mo$_5$SiB$_2$ are brittle phases. For a given α-Mo volume fraction, the room temperature fracture can be dramatically improved by making the α-Mo a continuous "binder" phase instead of small, isolated particles. The creep strength can be dramatically improved by solid solution alloying. Again, for a given α-Mo volume fraction, the control of the microstructural scale and morphology is of critical importance. The compositional and microstructural design of Mo-Si-B alloys involves a trade-off between the simultaneous demands for adequate oxidation resistance, fracture toughness and creep strength. While the Mo-

Si-B system is unique in the sense that it can deliver solutions to each of these demands, further work is needed to optimize both composition and microstructure such that all three requirements are satisfied at the same time.

REFERENCES

1. Y. Yamabe-Mitarai, "High-temperature strength of Ir-based refractory superalloys," Mat. Res. Soc. Symp. Proc. Vol. 646, J. H. Schneibel et al., eds., pp. N3.6.1-3.6.12.

2. A. K. Vasudévan and J. Petrovic, "A comparative overview of molybdenum silicide composites," Mater. Sci. and Engng. A155 (1992) 1-17.

3. M. K. Meyer, M. J. Kramer, and M. Akinca [sic], "Compressive creep behavior of Mo_5Si_3 with the addition of boron," Intermetallics 4 (1996) 273-281.

4. M. Akinc, M. K. Meyer, M. J. Kramer, A. J. Thom, J. J. Huebsch, and B. Cook, "Boron-doped molybdenum silicides for structural applications," Intermetallics A261 (1999) 16-23.

5. M. K. Meyer, A. J. Thom, and M. Akinc, "Oxide scale formation and isothermal oxidation behavior of Mo-Si-B intermetallics at 600-1000°C," Intermetallics 7 (1999) 153-162.

6. H. Nowotny, E. Kimakopoulou, and H. Kudielka, Mh. Chem. 88 (1957) 180-192.

7. D. M. Berczik, United States Patent 5,595,616 (1997), "Method for enhancing the oxidation resistance of a molybdenum alloy, and a method of making a molybdenum alloy."

8. D. M. Berczik, United States Patent 5,693,156 (1997), "Oxidation Resistant Molybdenum Alloys."

9. R. Raj and L. R. Thompson, "Design of the microstructural scale for optimum toughening in metallic composites," Acta Metall. Mater. 42 (1994) 4135-4142.

10. I. Rosales and J. H. Schneibel, "Stoichiometry and mechanical properties of Mo_3Si," Intermetallics 8 (2000) 885-889.

11. S. V. Raj, J. D. Whittenberger, B. Zeumer, and G. Sauthoff, "Elevated temperature deformation of Cr_3Si alloyed with Mo," Intermetallics 7 (1999) 743-755.

12. R. D. Field, D. J. Thoma, J. C. Cooley, F. Chu, C. L. Fu, M. H. Yoo, W. L. Hults, C. M. Cady, "Dislocations in Mo_5SiB_2 T2 Phase," Intermetallics 9 (2001) 863-868

13. C. L. Fu, X. Wang, Y. Y. Ye, & K. M. Ho, "Phase stability, bonding mechanism, and elastic constants of Mo_5Si_3 by first-principles calculation," Intermetallics, 7 (1999) 179-184.

14. J. H. Schneibel, C. J. Rawn, T. R. Watkins, and E. A. Payzant , "Thermal expansion anisotropy of ternary molybdenum silicides based on Mo_5Si_3," Phys. Rev. B 65 (2002)134112

15. J. H. Schneibel, M. J. Kramer, Ö. Ünal, and R. N. Wright, "Processing and mechanical properties of a molybdenum silicide with the composition Mo-12Si-8.5B (at. %)," Intermetallics 9 (2001) 25-31.